Chapter 12

Multimode Waveguides on an SOI Platform for Arbitrary Power Splitting Ratio Couplers

Trung-Thanh Le and Duy-Tien Le

Additional information is available at the end of the chapter

http://dx.doi.org/10.5772/intechopen.76799

Abstract

Optical power couplers with arbitrary power splitting ratios are important components for many applications such as Mach-Zehnder interferometer-based structures, filters, switches, dispersion compensations, optical interconnects, and microring resonators. In this chapter, we present a new approach to achieve a very high compact coupler with arbitrary power splitting ratios on silicon on insulator (SOI) waveguides. The proposed device requires only one 4×4 multimode interference (MMI) coupler. We use a passive wide SOI waveguide to achieve the phase shifter. The footprint of the whole device is only about 6×150 μm^2. A large fabrication tolerance of ±50 nm can be achieved. The modified effective index method, beam propagation method, finite difference method, and finite difference-time difference method are used to optimally design the whole device.

Keywords: multimode interference, silicon on insulator, multimode waveguide, finite difference-time difference, finite difference method, modified effective index method

1. Introduction

Integrated optical couplers with arbitrary power coupling ratios are important components in optical communication applications. Such couplers can be used in Mach-Zehnder interferometer (MZI) structures, power taps, and microring resonators, and so on. In principle, any power coupling ratio can be achieved for standard 2×2 directional couplers [1]. The power coupling ratios can be controlled by adjusting the coupling length and/or the gap between the two waveguides of the directional coupler [2]. In practice, accurate fabrication of the gap requires

very tight control of the fabrication process. Moreover, additional loss due to mode conversion loss has been found to be a problem [3].

A multimode interference (MMI) power splitter plays an important role in the development of integrated photonics due to large fabrication tolerance, wide operation bandwidth, and compact size. Therefore, MMI couplers with unequal power splitting ratios have been found in many applications such as optical monitoring, optical microring resonators [4, 5], and optical reflectors [6]. In order to achieve a coupler with a variable power splitting ratios, a Mach-Zehnder interferometer (MZI) with a phase shifter at the arm can be used [7–11]. With a conventional MMI coupler with a rectangular shape, it has been shown that such device can only provide limited splitting ratios and therefore it has limited applications in all-optical signal processing and optical networks.

In the literature, there are some methods for obtaining variable power optical couplers based on MMI structures such as butterfly-like MMIs [12], exponential MMIs [13, 14], and angled MMIs [15, 16]. However, these methods require a very complicated fabrication processes, and they have a low fabrication tolerance. In addition, these methods are not suitable for silicon photonics because of high losses.

In recent years, we have presented some methods to overcome the limitations of the previous approaches such as by cascading three or four MMI couplers [17], using an MZI structure with a multimode waveguide [18], using slot waveguide [19]. Other approaches are to use MMI structure with QR code-like nanostructure [20, 21] or double MMI coupler [22]. However, such approaches still require a quite complex fabrication process and they have a large footprint.

In this chapter, we present a new approach to achieve a 2×2 coupler based on only one 4×4 MMI coupler with wide waveguide on silicon on insulator waveguides. Our new method has advantages of compact size, ease of fabrication with the current CMOS circuitry.

2. Theory of MMI matrix

Multimode interference coupler includes three regions: single mode input, output waveguides, and multimode waveguide connecting with two input and output regions. The multimode region has a large width to support some modes. The operation of the MMI coupler is based on Talbot effect [4, 23]. Based on locations of input field excitations, there are three main interference mechanisms: (1) general interference (GI) mechanism, which is independent of the modal excitation; (2) restricted interference (RI) mechanism, in which excitation inputs are placed at some special positions so that certain modes are not excited; (3) symmetric interference (SI) mechanism, in which the excitation input is located at the center of the multimode section.

An NxN GI-MMI coupler has length $L = L_{MMI} = \frac{p}{N} 3L_{\pi}$, where p is a positive integer such that p and N are without a common divisor. In practical designs, the shortest devices are obtained for p = 1. The resulting amplitudes from image input i (i = 1,…,N) to output j (j = 1,…,N) can be given in a compact form [23].

$$A_{ij} = A_{ji} = \sqrt{\frac{1}{N}} \tag{1}$$

where $|A_{ij}|^2$ is the normalized power of the output images. The phases ϕ_{ij} of the equal output signals at the output waveguides can be calculated by [23]: for i + j: even, $\phi_{ij} = \phi_0 + \pi + \frac{\pi}{16}(j-i)(8-j+i)$ and for i + j: odd, $\phi_{ij} = \phi_0 + \frac{\pi}{16}(i+j-1)(8-j-i+1)$; where the input ports i (i = 1, 2,…,N) are numbered from bottom to top and the output ports j (j = 1, 2,…, N) are numbered from top to bottom in the MMI coupler. $\phi_0 = -\beta_0 L_{MMI} - \frac{\pi}{2}$ is a constant phase that depends upon the MMI geometry and therefore can be implied in the following calculations.

In this chapter, the access waveguides are identical single mode waveguides with width W_a. The input and output waveguides are located at [24].

$$\mathrm{x} = \left(i + \frac{1}{2}\right)\frac{W_{MMI}}{N} \tag{2}$$

The electrical field inside the MMI coupler can be expressed by [25].

$$E(x,z) = \exp(-jkz)\sum_{m=1}^{M} E_m \exp\left(j\frac{m^2\pi}{4\Lambda}z\right)\sin\left(\frac{m\pi}{W_{MMI}}x\right) \tag{3}$$

We showed that the characteristics of an MMI device could be described by a transfer matrix [2]. This transfer matrix is a very useful tool for analyzing cascaded MMI structures. The phase ϕ_{ij} associated with imaging an input i to an output j in an MMI coupler. These phases ϕ_{ij} form a matrix $\mathbf{\Phi}$, with i representing the row number, and j representing the column number. Then the transfer matrix of the MMI coupler $\mathbf{M}$ is directly related to $\mathbf{\Phi}$, and the output field distribution emerging from the MMI coupler can be written as

$$\mathbf{b} = \mathbf{M}\mathbf{a} \tag{4}$$

where $\mathbf{a} = [a_1\ \mathrm{a}_2 \ldots \mathrm{a}_N]^T$, $\mathbf{b} = [b_1\ \mathrm{b}_2 \ldots \mathrm{b}_N]^T$ and $\mathbf{M} = \left[m_{ij}\right]_{NxN}$. The superscript T indicates the transpose of a matrix. a_i(i = 1,…,N) is the complex field amplitude at input waveguide i and b_j (j = 1,…,N) is the complex field amplitude at output waveguide j. Elements of the transfer matrix $\mathbf{M}$ are $m_{ij} = m_{ji} = A_{ij}e^{j\phi_{ij}}$, where A_{ij} is the field amplitude transfer coefficient and ϕ_{ij} is the phase shift when imaging from input i to output j.

Here, we propose a 4×4 MMI coupler with a width of W_{MMI}, length of L_{MMI}. A single 4×4 MMI coupler at a length of $L_1 = \frac{3L_\pi}{4}$ is described by the following transfer matrix [26–28].

$$\mathbf{M} = \frac{1}{2}\begin{bmatrix} -1 & -e^{j\frac{3\pi}{4}} & e^{j\frac{3\pi}{4}} & -1 \\ -e^{j\frac{3\pi}{4}} & -1 & -1 & e^{j\frac{3\pi}{4}} \\ e^{j\frac{3\pi}{4}} & -1 & -1 & -e^{j\frac{3\pi}{4}} \\ -1 & e^{j\frac{3\pi}{4}} & -e^{j\frac{3\pi}{4}} & -1 \end{bmatrix} \tag{5}$$

If the length is doubled to $L_{MMI} = 2L_1 = 3L_\pi/2$, a new 4×4 MMI coupler is formed and its transfer matrix is

$$\mathbf{S} = (\mathbf{M})^2 = \frac{1}{2}\begin{bmatrix} 1-j & 0 & 0 & 1+j \\ 0 & 1-j & 1+j & 0 \\ 0 & 1+j & 1-j & 0 \\ 1+j & 0 & 0 & 1-j \end{bmatrix} \tag{6}$$

3. Modified effective index and numerical methods

In this chapter, we use our proposed modified effective index method (MEIM) for designing MMI structures based on silicon waveguides as shown in [29]. The principle of this MEIM is to use the beat length L_π of the MMI coupler as the invariant. Here, the beat length of an MMI structure can be defined as $L_\pi = \pi/(\beta_0 - \beta_1)$, where β_0 and β_1 are the propagation constants of the fundamental and first order modes, respectively. We shall find a matching value of the cladding index for the effective index method that forces the beat length L_π in the equivalent 2D model to be equal to the beat length in an accurate 3D model. By this way, we find an optimal effective cladding index. For our silicon waveguide structure, in this chapter, we found that equivalent effective indices of the core waveguide and the cladding waveguide are to 2.82 and 2.19, respectively.

In order to optimally design the MMI coupler, we use the beam propagation method (BPM). We showed that the width of the MMI is optimized to be W_{MMI} = 6 μm for compact and high performance device. **Figure 1** shows numerical simulations at optimal MMI length of $L_{MMI} = 141.7\ \mu m$ for signal at input port 1 and at input port 2. The simulations show that a very low insertion loss of 0.7 dB for both cases [2].

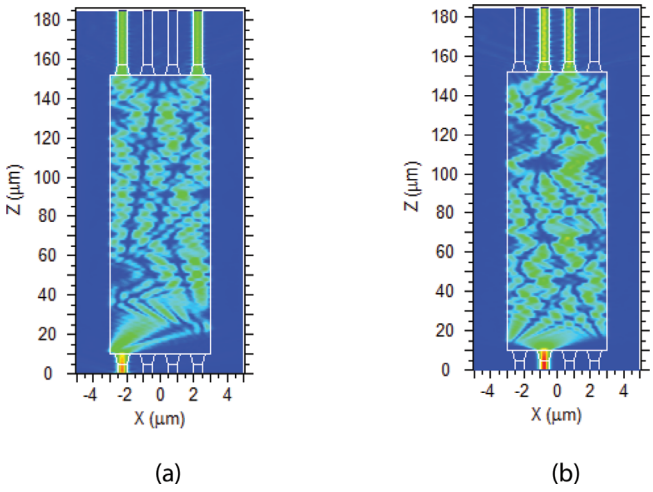

Figure 1. Power splitting ratio scheme based on 4×4 MMI coupler (a) Input 1 and (b) Input 2.

4. Arbitrary splitting ratio coupler based on a 4×4 MMI coupler

Figure 2 shows the new scheme for achieving arbitrary coupling ratios in only one 4×4 MMI structure. We use two waveguides with different widths $W_{co1} = 300nm$ and $W_{co2} = 500nm$ at the two arms of the structure. The cross-sectional view of the SOI waveguide is shown in **Figure 3**. Here, the height of the SOI waveguide $h_{co} = 220nm$, the width of the SOI waveguide varies from 300 nm to 500 nm for single mode operation at wavelength of 1550 nm.

By using the FDM method, the effective refractive index of the SOI waveguide at different waveguide width of 300 nm to 500 nm can be calculated as shown in **Figure 4**. As an example, **Figure 5** shows the mode profile for the waveguide at the width of 300 nm and 500 nm, respectively.

A change in the effective index will induce the change in the phase shift. The phase difference between two waveguide then can be expressed by [30].

$$\Delta\varphi = \frac{2\pi}{\lambda}\Delta n_{eff} L_{arm} \tag{7}$$

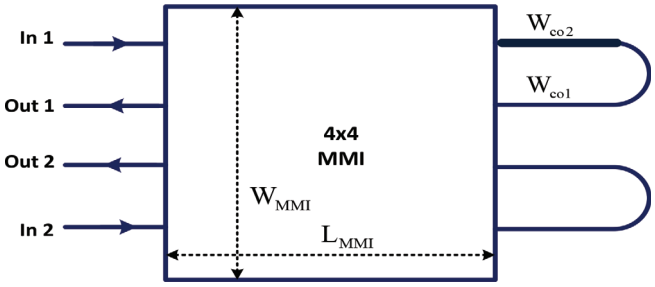

Figure 2. Power splitting ratio scheme based on 4×4 MMI coupler.

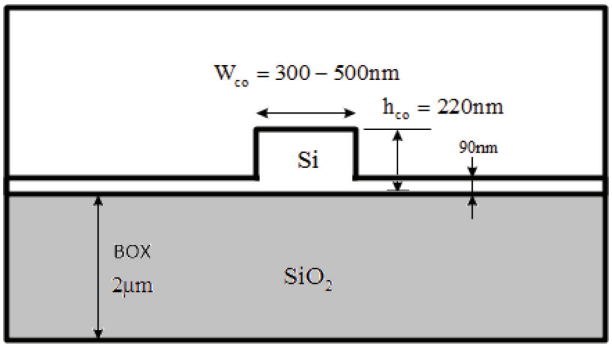

Figure 3. SOI waveguide structure.

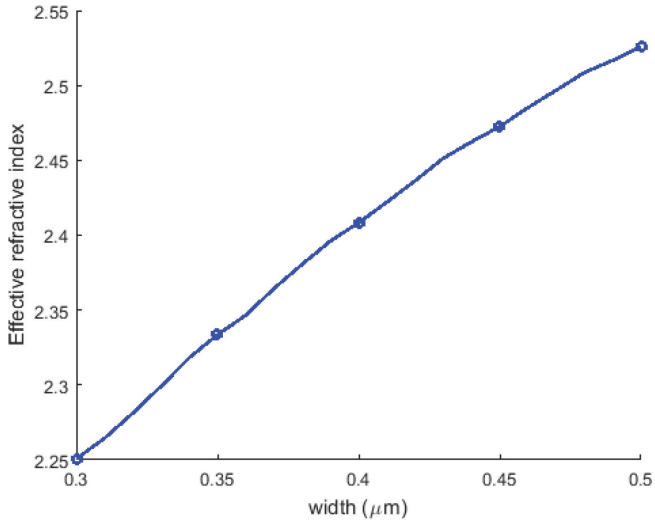

Figure 4. Effective refractive index of the SOI waveguide calculated by the FDM.

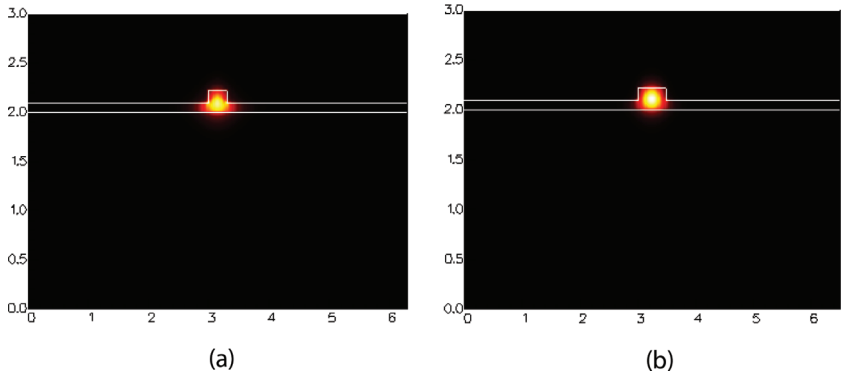

Figure 5. Field profile of the SOI waveguide (a) width of 300 nm and (b) width of 500 nm.

where Δn_{eff} is the difference in the effective index, L_{arm} is the length of the waveguide with the width of W_{co2}. As a result, the length of the waveguide W_{co2} to achieve the phase shift from 0 to π is presented in **Figure 6**. We see that the short length of 3.5035 μm is required to achieve a phase shift of π.

Due to the phase shift $\Delta\varphi$, the complex amplitudes at the input ports and output ports of the coupler of **Figure 2** can be described in terms of cascaded transfer matrices as

$$\mathbf{S} = \frac{1}{\sqrt{2}}\begin{bmatrix} 1 & j \\ j & 1 \end{bmatrix}\begin{bmatrix} e^{j\Delta\varphi} & 0 \\ 0 & 1 \end{bmatrix}\frac{1}{\sqrt{2}}\begin{bmatrix} 1 & j \\ j & 1 \end{bmatrix} = e^{j\frac{\Delta\varphi}{2}}\begin{bmatrix} \tau & \kappa \\ \kappa^* & -\tau^* \end{bmatrix} \tag{8}$$

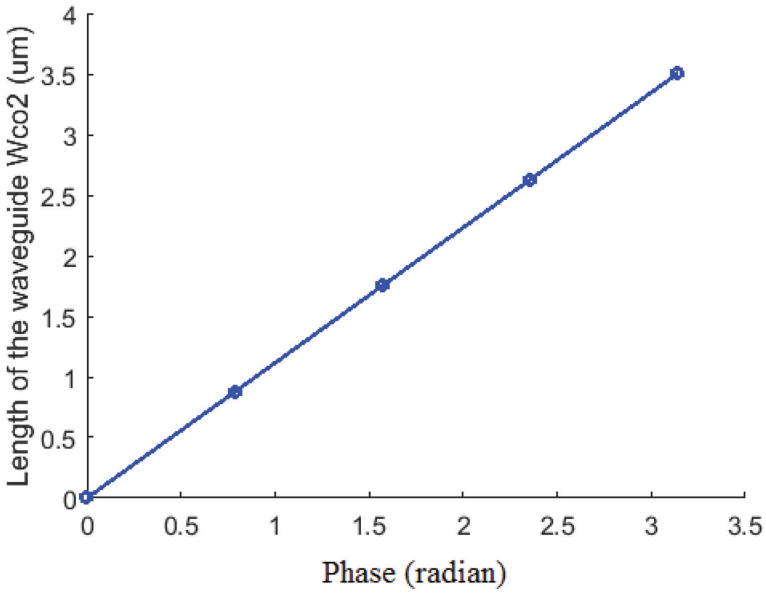

Figure 6. Length of the waveguide Wco2 required to achieve the phase shift from 0 to π.

where $\tau = \sin\left(\frac{\Delta\varphi}{2}\right)$, and $\kappa = \cos\left(\frac{\Delta\varphi}{2}\right)$. Therefore, if an input signal having power presented at input port 1 of the coupler in **Figure 2**, the normalized powers at output port 1 and output port 2 can be expressed by:

$$Out_1 = \sin^2\left(\frac{\Delta\varphi}{2}\right), \text{and } Out_2 = \cos^2\left(\frac{\Delta\varphi}{2}\right) \tag{9}$$

From Eqs. (7) and (9), the normalized output powers can be calculated and plotted in **Figures 7** and **8**. It is showed that any power splitting ratio can be achieved by changing the phase shift from 0 to π or changing the length of the Wco2 waveguide from 0 to 3.51μm.

Consider the length of the Wco2 waveguide variation, the normalized output powers are shown in **Figure 9**. The simulation shows that the changes in normalized output powers are very small (nearly 0% in the range of −50 nm to +50 nm). It is feasible for the current CMOS circuitry [31].

Finally, we use FDTD method to simulate our proposed structure and then make a comparison with the analytical theory. In our FDTD simulations, we take into account the wavelength dispersion of the silicon waveguide. We employ the design of the MMI coupler presented in the previous section. A continuous light pulse of 15 fs pulse width is launched from the input to investigate the transmission characteristics of the device. The grid size $\Delta x = \Delta y = 20nm$ and $\Delta z = 20nm$ are chosen in our simulations. The FDTD simulations for the whole device are shown in **Figure 10**.

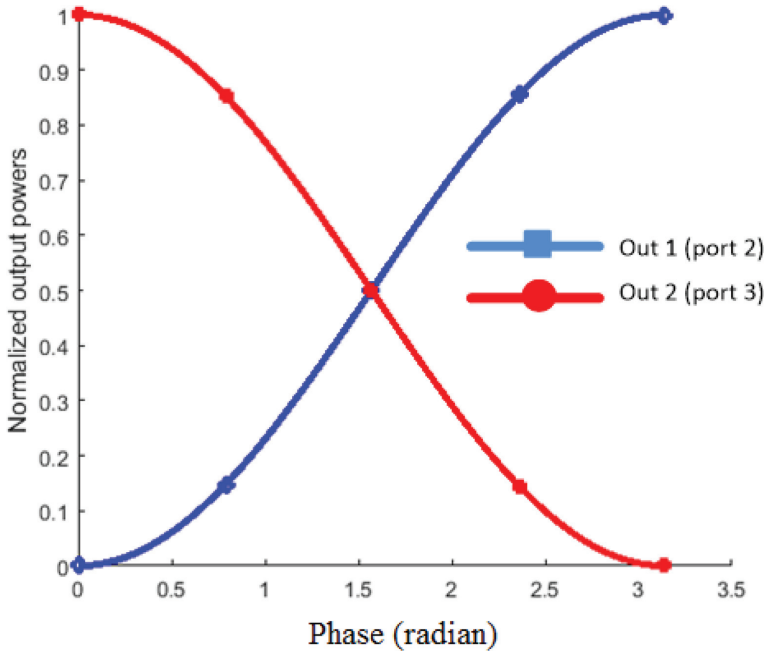

Figure 7. Normalized output powers at ports 2 (out1) and 3 (out2) for different phase shifts.

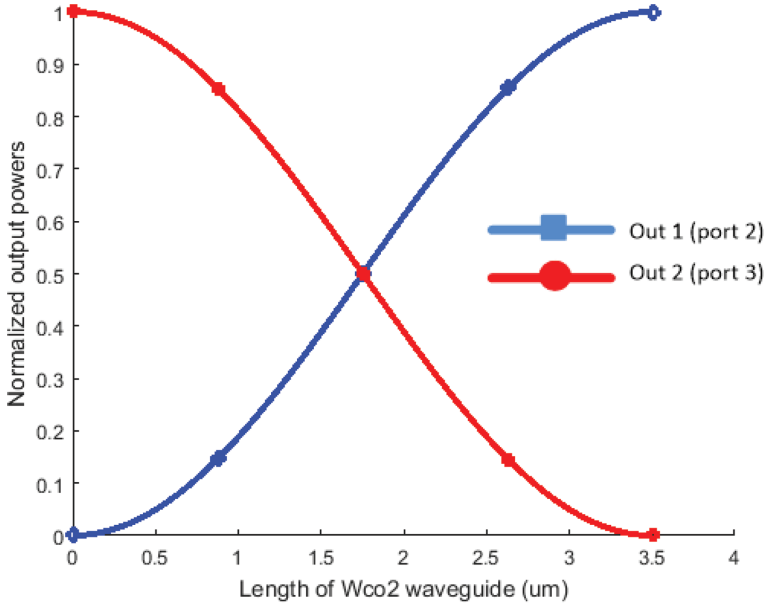

Figure 8. Normalized output powers at ports 2 and 3 for different Wco2 lengths.

http://dx.doi.org/10.5772/intechopen.76799

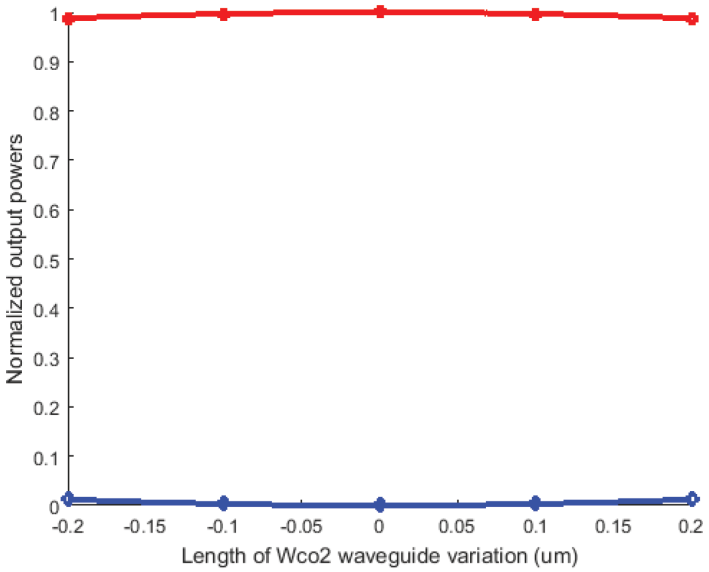

Figure 9. Normalized output powers at ports 2 and 3 for different Wco2 length variation.

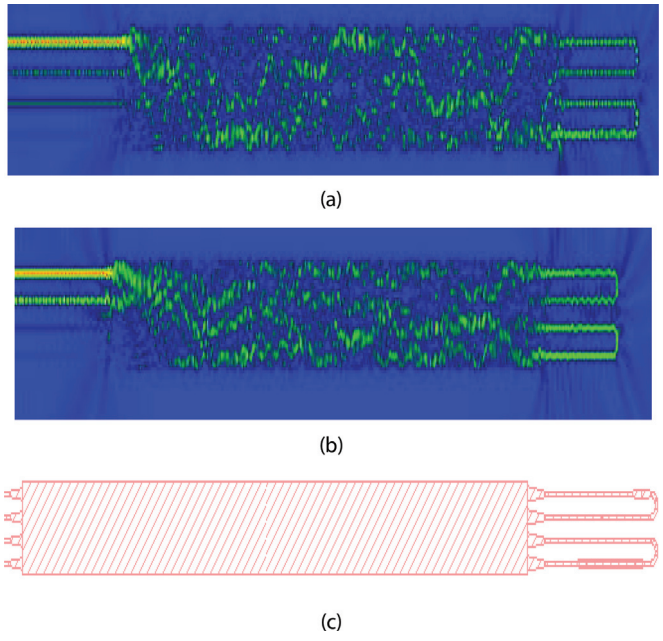

Figure 10. Optical field propagation through the coupler for input signal presented at port 1 and for length of the Wco2, (a) 1.75 μm and (b) 3.51 μm, and (c) mask design.

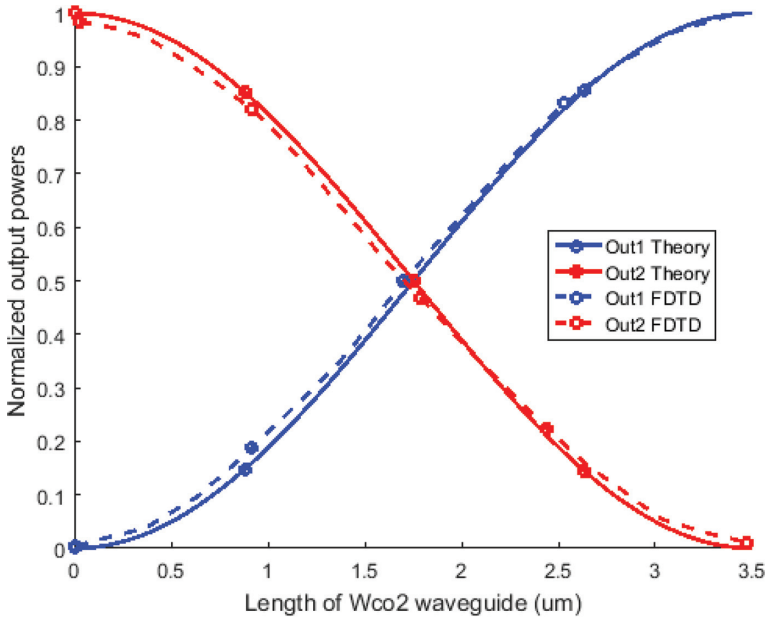

Figure 11. FDTD simulations compared with the theoretical analysis at different lengths of the Wco2 waveguide.

Figure 11 shows the FDTD simulations compared with theoretical analysis. The simulations show that the device operation has a good agreement with our prediction by analytical theory.

5. Conclusions

We presented a compact structure with a footprint of 6×150 μm^2 based on silicon on insulator waveguides for 2×2 couplers with free of choice power splitting ratios. The new structure requires only one 4×4 multimode interference coupler. The wide SOI waveguide is used to achieve the phase shift. By changing the length of the wide waveguide from 0 to 3.51 μm, any power splitting ratios can be achieved. The device operation has been verified by using the FDTD. This coupler can be useful for optical interconnects, microring resonator applications.

Author details

Trung-Thanh Le* and Duy-Tien Le

*Address all correspondence to: thanh.le@vnu.edu.vn

Vietnam National University (VNU), International School (VNU-IS), Hanoi, Vietnam

References

[1] Payne F. Design principles of ring resonator waveguide devices. Private Communication. 2007

[2] Le T-T. Multimode Interference Structures for Photonic Signal Processing. Germany: LAP Lambert Academic Publishing; 2010

[3] Xia F, Sekaric L, Vlasov YA. Mode conversion losses in silicon-on-insulator photonic wire based racetrack resonators. Optics Express. 2006;**14**:3872-3886

[4] Soldano LB, Pennings ECM. Optical multi-mode interference devices based on self-imaging: Principles and applications. IEEE Journal of Lightwave Technology. 1995;**13**: 615-627

[5] Suzuki S, Kazuhiro O, Yoshinori H. Integrated-optic double-ring resonators with a wide free spectral range of 100 GHz. Journal of Lightwave Technology. 1995;**13**:1766-1771

[6] Jeong S, Matsuo S, Yoshikuni Y, et al. Flat-topped spectral response in a ladder-type interferometric filter. IEICE Transactions on Electronics. 2005;**E88-C**:1747-1754

[7] Oguma M, Jinguji K, Kitoh T, et al. Flat-passband interleave filter with 200 GHz channel spacing based on planar lightwave circuit-type lattice structure. Electronics Letters. 2000; **36**:1299-1300

[8] Takiguchi K, Jinguji K, Okamoto K, et al. Variable group-delay dispersion equalizer using lattice-form programmable optical filter on planar. IEEE Journal of Selected Topics in Quantum Electronics. 1996;**2**:270-276

[9] Yariv A. Critical coupling and its control in optical waveguide-ring resonator systems. IEEE Photonics Technology Letters. 2002;**14**:483-485

[10] Choi JM, Lee RK, Yariv A. Control of critical coupling in a ring resonator–fiber configuration: Application to wavelength-selective switching, modulation, amplification, and oscillation. Optics Letters. 2001;**26**:1236-1238

[11] Takiguchi K, Jinguji K, Ohmori Y. Variable group-delay dispersion equaliser based on a lattice-formprogrammable optical filter. Electronics Letters. 1995;**31**:1240-1241

[12] Besse PA, Gini E, Bachmann M, et al. New 2×2 and 1×3 multimode interference couplers with free selection of power splitting ratios. IEEE Journal of Lightwave Technology. 1996; **14**:2286-2293

[13] Dai D, He S. Proposal for diminishment of the polarization-dependency in a Si-nanowire multimode interference (MMI) coupler by tapering the MMI section. IEEE Photonics Technology Letters. 2008;**20**:599-601

[14] Dai D, He S. Design of an ultrashort Si-nanowaveguide-based multimode interference coupler of arbitrary shape. Applied Optics. 2008;**47**:38-44

[15] Levy DS, Li YM, Scarmozzino R, et al. A multimode interference-based variable power splitter in GaAs-AlGaAs. IEEE Photonics Technology Letters. 1997;**9**:1373-1375

[16] Lai Q, Bachmann M, Hunziker W, et al. Arbitrary ratio power splitters using angled silica on siliconmultimode interference couplers. Electronics Letters. 1996;**32**:1576-1577

[17] Truong C-D, Le T-T. Power splitting ratio couplers based on MMI structures with high bandwidth and large tolerance using silicon waveguides. Photonics and Nanostructures - Fundamentals and Applications. 2013;**11**:217-225

[18] Le TT, Cahill LW, Elton D. The design of 2×2 SOI MMI couplers with arbitrary power coupling ratios. Electronics Letters. 2009;**45**:1118-1119

[19] Le TT and Cahill LW. The design of multimode interference couplers with arbitrary power splitting ratios on an SOI platform. In LEOS 2008, Newport Beach, California, USA, 9-14 Nov 2008

[20] Ke X, Liu L, Wen X, et al. Integrated photonic power divider with arbitrary power ratios. Optics Letters. 2017;**42**:855-858

[21] Piggott AY, Petykiewicz J, Su L, et al. Fabrication-constrained nanophotonic inverse design. Scientific Reports. 2017;**7**:1786

[22] Cherchi M, Ylinen S, Harjanne M, et al. Unconstrained splitting ratios in compact double-MMI couplers. Optics Express. 2014;**22**:9245-9253

[23] Bachmann M, Besse PA, Melchior H. General self-imaging properties in N × N multimode interference couplers including phase relations. Applied Optics. 1994;**33**:3905-3911

[24] Le D-T, Le T-T. Coupled resonator induced transparency (CRIT) based on interference effect in 4×4 MMI coupler. International Journal of Computer Systems. 2017;**4**:95-98

[25] Heaton JM, Jenkins RM. General matrix theory of self-imaging in multimode interference (MMI) couplers. IEEE Photonics Technology Letters. 1999;**11**:212-214

[26] Le T-T. Two-channel highly sensitive sensors based on 4 × 4 multimode interference couplers. Photonic Sensors. 2017;**7**:357-364

[27] Le T-T, Cahill L. The design of 4×4 multimode interference coupler based microring resonators on an SOI platform. Journal of Telecommunications and Information Technology. 2009:98-102

[28] Le DT, Do DT, Nguyen VK, et al. Sharp asymmetric resonance based on 4×4 multimode interference coupler. International Journal of Applied Engineering Research. 2017;**12**: 2239-2242

[29] Le T-T. An improved effective index method for planar multimode waveguide design on an silicon-on-insulator (SOI) platform. Optica Applicata. 2013;**43**:271-277

[30] Petrone G, Cammarata G. Modelling and Simulation. Rijeka: InTech Publisher; 2008

[31] Dan-Xia X, Schmid JH, Reed GT, et al. Silicon photonic integration platform—Have we found the sweet spot? IEEE Journal of Selected Topics in Quantum Electronics. 2014;**20**: 8100217